The Test and Analysis of a 3—Stage Reconnection Coilgun

Shun—Shou Gao and Cheng—Wei Sun

Southwest Institute Of Fluid Physics, P. O. Box523, Chengdu, 610003, China

Phone 86 816 2484051, Fax 86 816 2272695, Email dingbn@Sun. ihep. ac. cn

Ying—Min Zhu, Jian—Jun Cheng and De—Man Wang

P. O. Box 187, Xidian University, Xi'an, 710071, China

Phone 86 29 8228300 ext. 3064, Fax 86 29 8232281, Email XDU@Xidian. edu. cn

Abstract — For the principle test a 3—stage reconnection coilgun was built. It has a 64mm bore, length of 330mm and a projectile weight of 1kg. The muzzle velocity is about 100m/s. The value of the capacitors of the driver coils are 4480, 3000 and 715μF with initial voltages 3. 3, 3. 6 and 6. 0 kV respectively. The agreement of the results between the test and the analysis is good. The performances of AC and DC work modes are compared. DC mode means that a shunt circuit is inserted into each driver coil circuit to prevent current reveral. In the test, visible plastic deformations of the armature occur and it was confirmed by computer simulation.

Index Terms — AC and DC work modes, Coilgun, Plastic deformations, System analysis.

I 3—STAGE RECONNECTION COILGUN

For the principle test a 3—stage reconnection coilgun was built in 1995—1997. Each stage has a 64mm bore, a length of 100mm and built of a flat electromagnetic winding wire. There is a 30mm interstage space between coils. Each coil has 42 turns divided into 3 layers and is energized by capacitors, Fig. 1—1. Several kinds of projectiles are adopted, each has a weight of 1kg, a 60mm outer diameter, and an armature length of 165mm, 220mm respectively, Fig. 1—2, The armature sleeve is made of aluminium alloy. The stage velocities of the projectile are measured by laser velocity—measuring—transducer. The laser transmitters and pickoff units are installed between the coils. The laser signals are sent to the photoelectric commutator by optical cable, and then, the converted electrical signals are sent to the data—processing system which furnishes both the value of the projectilevelocity and the delay signal for firing of the next stage. Another velocity transducer is placed after the last stage to measure the muzzle velocity.

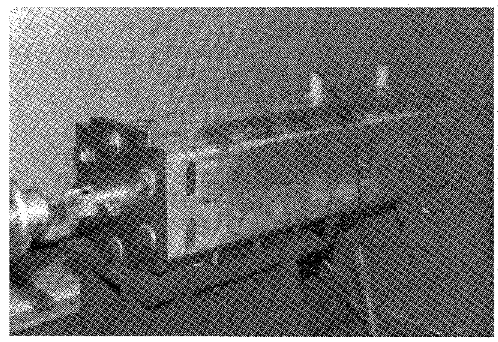

Fig. 1—1 The 3—stage coilgun

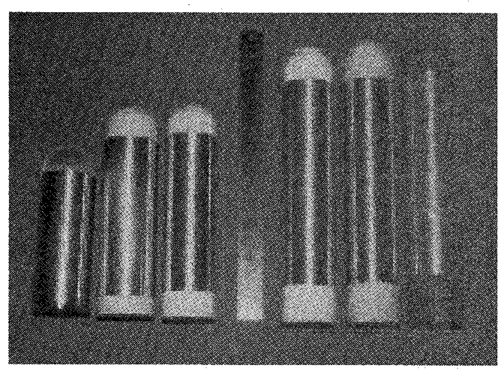

Fig. 2 The projectiles (armatures and their payload) in the coilgun

This project supported by National Natural Science Foundation of China, 19482004

The systems analysis equations are [1]

$$
\begin{aligned}
&([L]+[M])\frac{\mathrm{d}}{\mathrm{d}t}\{I\} \\
&=\{V_c^*\}-[R]\{I\}-v\left(\frac{\mathrm{d}}{\mathrm{d}x}[M]\right)\{I\} \\
&[C]\frac{\mathrm{d}}{\mathrm{d}t}\{V_c\}=-\{I_d\} \qquad (1)\\
&m_0\frac{\mathrm{d}v}{\mathrm{d}t}=\sum\sum I_d I_p\frac{\mathrm{d}M_{pd}}{\mathrm{d}x} \\
&\frac{\mathrm{d}x}{\mathrm{d}t}=v
\end{aligned}
$$

Where $\{I\}=[[I_d]^T,[I_p]^T]^T$, $[I_d]$are currents in coils and $[I_p]$are currents in the armature piece circuits; $\{V_c^*\}=[[V_c]^T,[0]^T]$, $\{V_c\}$are voltages of capacitors in coil loops and m zeroes shows that there are no capacitor in the armature piece circuits; L, M are the self and mutual inductances of the coils and armature pieces respectively which have been calculated referring to [2]. m_0, v, x are the mass, velocity and position.

The results of the test and simulative analysis are listed in Tab. I. Their agreement is quite good. Because of lack of funds, only one coilgun was built at a time. The 1st, 2nd and 3rd stage coilguns were built successively and the corresponding tests were made respectively. Since the capacitors for the 2nd stage gun were not available, we used the same capacitors as for a single stage gun. The calculated results of the drive coil currents, voltages and the projectile displacement, velocity and acceleration are given in Fig. 1—3, 1—4 and 1—5. The measuring signal of the muzzle velocity of the projectile is given in Fig. 1—6. The photo shows that the projectile passes two laser transducers sucessively. The distance between the transducers is 10mm. In the abscissa of the figure, each small graduation is 10μs and the big one is 50μs. According to the measuring signal, we can calculate the muzzle velocity of the projectile is about 100m/s.

Tab. I MEASURED AND CALCULATED MUZZLE VELOCITIES OF THE 1ST STAGE, 2ND STAGE AND 3RD STAGE COILGUN

Parameters Stage	Capacitances (μF)	Initial Charge (kV)	Velocities (m/s) Measured	Calculated
1	2073	3.0	22.00	22.31
2	2073, 2073	4.0, 4.0	60.45	66.00
3	4480, 3000, 715	3.3, 3.6, 4.0	100.00	104.00

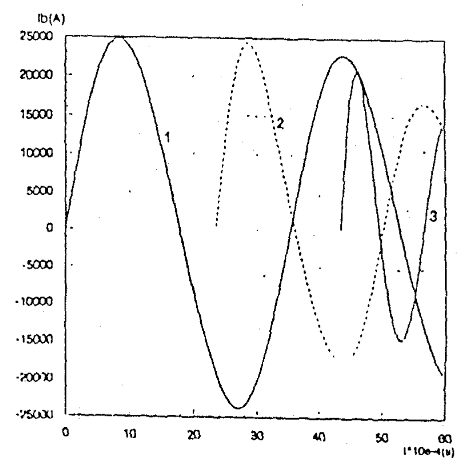

Fig. 1—3 The coil currents I_{bi} in 3—stage coilgun

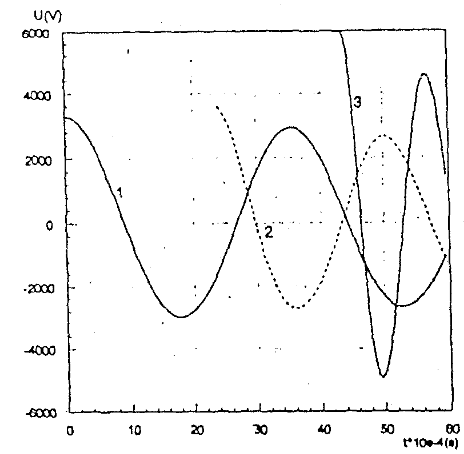

Fig. 1—4 The coil voltages U_i in 3—stage coilgun

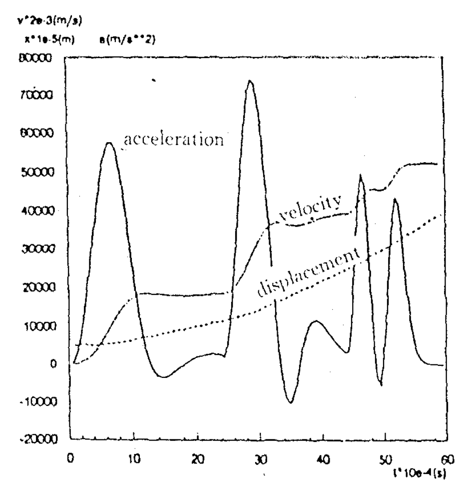

Fig. 1—5 The projectile displacement, velocity and acceleration in 3—stage coilgun

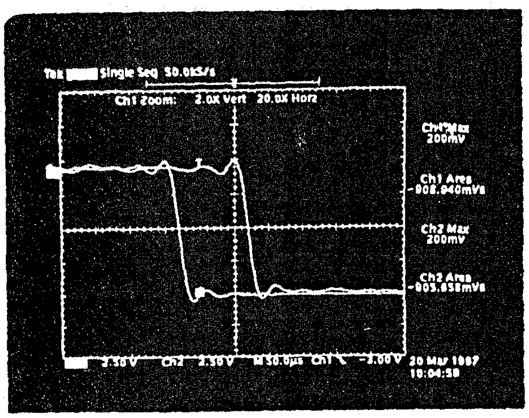

Fig. 1—6 The measuring signals of the muzzle velocity in 3—stage coilgun

Ⅱ COMPARISON OF AC AND DC WORK MODES

The driver coil circuit is an L—C circuit and its current is AC when the capacitor discharges to the coil directly. The relationship between the phase and the amplitude of the currents in the coils, I_d, and those of the induced current in the armature, I_p, is complex, Eq. 1. The projectile is accelerated when the I_d and I_p are in the anti—phase and the decelerated sometimes when the I_d and I_p are in the same—phase. That makes the acceleration of the projectile fluctuate heavily. A crowbar is added in the coil circuit[3]. Under given conditions the crowbar prevents reversal of the I_d, and the system works in a DC mode, Fig. 2—1. In another paper[4], the system equations of a DC mode were derived exhaustively and mitigation in the acceleration fluctuation was shown. On the other hand, the AC mode raises the efficiency of the energy transformation because both the positive and the negative coil currents accelerate the projectile. The above fact has been demonstrated by the 3rd stage gun as follows.

For the 1st stage coilgun, the calculated projectile velocity curves for the AC and DC modes are given in Fig. 2—2. and 2—3 respectively. There are two velocity steps in AC mode. The first step approximately equals the velocity of the DC mode, and the second one shows that the negative half wave of the coil current further accelerates the projectile.

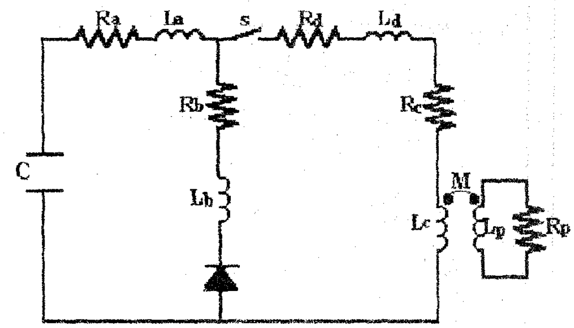

Fig. 2—1 The crowbar circuit in DC mode

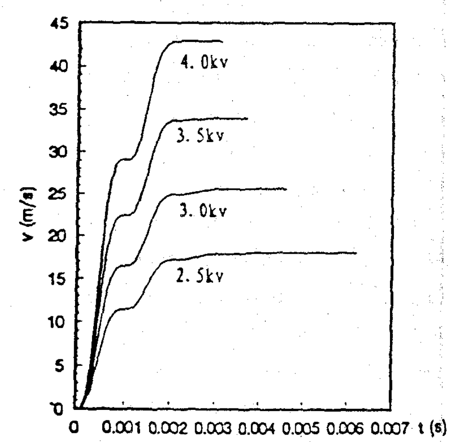

Fig. 2—2 The 1—stage coilgun, the calculated projectile velocities in AC mode

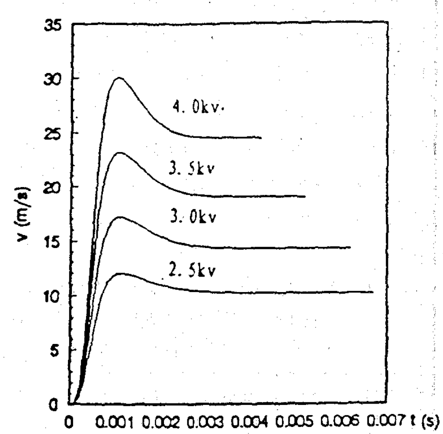

Fig. 2—3 The 1—stage coilgun, the calculated projectile velocities in DC mode

For the 2nd stage coilgun, the calculated and measured projectile velocities for AC and DC modes are given in Fig. 2—4 and 2—5, respectively. In the figures, the curves give the calculated values in each step and the ⊗ is the measured value. Since the projectile has already exited out of the barrel before the coil current reverses in the 2nd stage, the 2nd velocity step does not appear in Fig. 2—4.

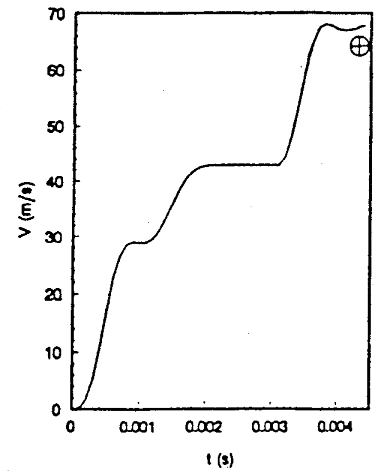

Fig. 2—4 The 2—stage coilgun, the calculated and measured projectile velocity in AC mode

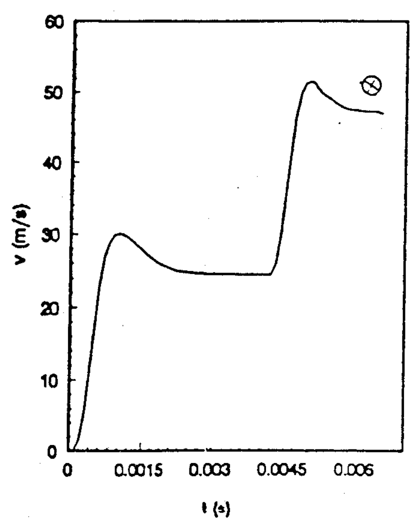

Fig. 2—5 The 2—stage coilgun, the calculated and measured projectile velocity in DC mode

Ⅲ THE MECHANICAL STRENGTH OF THE ARMATURE

Obvious plastic deformation appears at the tail of the armature in the test of the 1st stage coilgun, Fig. 3—1. The reasons are, (1) in aft pushing, the intensity of the magnetic field generated by the coil current is much stronger at the back of the projectile; (2) the induced current in the armature is not uniform axially and the current density in the tail is dominant. The radial pressure $f_r = JB_z$ at the tail is much greater, maybe several orders of magnitude, than in other parts of the projectile. Calculation was performed to analyse the armature deformation.

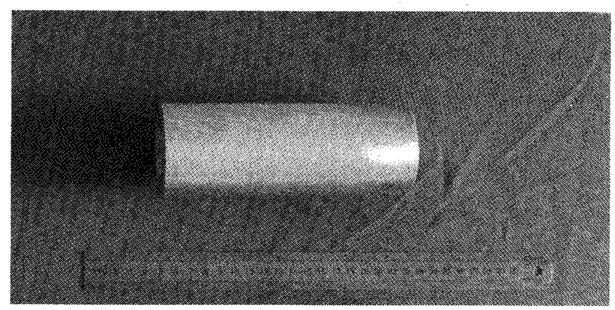

Fig. 3—1 The 1—stage coilgun, plastic deformation of the armature

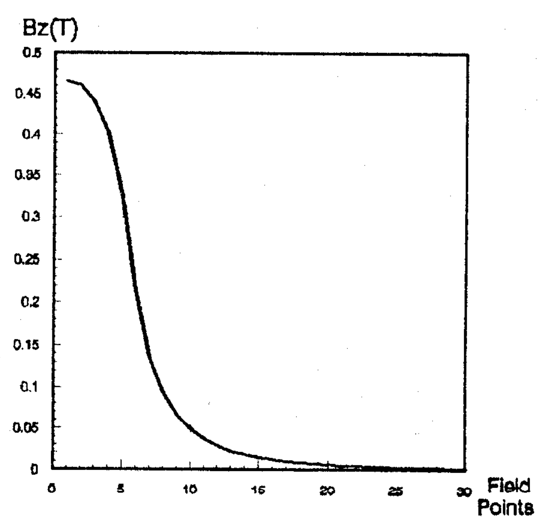

Fig. 3—2 The intensity of the 1—stage coilgun magnetic field when the coil current I_d is 1KA

The intensity of the magnetic field of the 1st stage coilgun is given in Fig. 3—2, when the coil current I_d is 1KA. The magnitude of I_d can be obtained from the simulation of the coilgun system. The instantaneous intensity of the magnetic field can be obtained using the I_d times the results in Fig. 3—2.

Since the induced azimuthal current in the armature is not uniform axially, in the simulating calculation, the armature was evenly discretized into 10 rings and the induced current in each ring, I_{pi}, is considered to be uniform, i=1, 2, …. The $I_{pi}(t)$ is obtained by the analysis. The I_{p1}, I_{p2}, I_{p3} and I_{p4} are given in Fig. 3—3 which shows that $I_{p1}(t)$ is much greater than the others. The $I_{pi}(t)$ after the 4th ring is much smaller and was not plotted.

In order to analyse the mechanical strength of the armature, a peak moment during the transmission was selected. At this moment, both the B_z at the tail of the armature and the $I_{p1}(t)$ have the largest values, so the product JB_z is the greatest. The instantaneous radial magnetic pressure on the armature can be calculated and the strength of the armature can be analysed.

This is a nonlinear problem of both material and geometry of elastoplasticity and the Super SAP (Structure Analysis Program) code is adopted for the calculation. When the deviation of the axes between the driver coil and the armature is ignored, all of the relevant parameters are axial symmetric about the centre line of the armature. For that axial symmetric mechanical problem, the armature is discretized into ring elements using a Finite Element Method (FEM). The elements and nodes are shown in Fig. 3—4. The boundary conditions are: the tail end is free and the front end is fixed because it is fastened to the the payload. The analysis results show that the first ten elements are in a plastic state, the 11th element is in an elastoplastic state and the others are in an elastic state. The radial displacements U_r of the outer and internal nodes are respectively given in Fig. 3—5 in which the maximum displacement is —7.32 in the 2nd node, and the outward is positive. Fig. 3—6 shows the armature deformation.

The intensity of magnetic field B_z is not uniform along the radial direction in the armature wall and increases from inside to outside. Because the outer B_z, which is

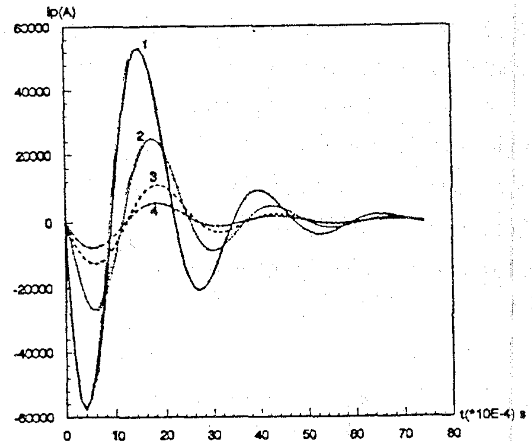

Fig. 3—3 The induced currents in the 1st—4th armature rings in the 1—stage coilgun

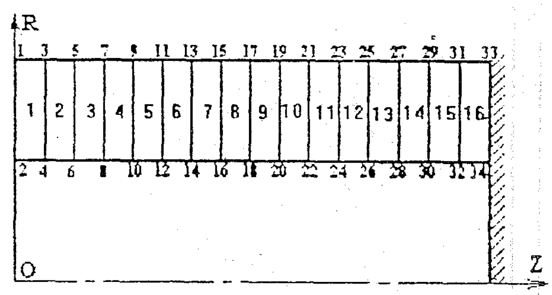

Fig. 3—4 The discretized armature elements

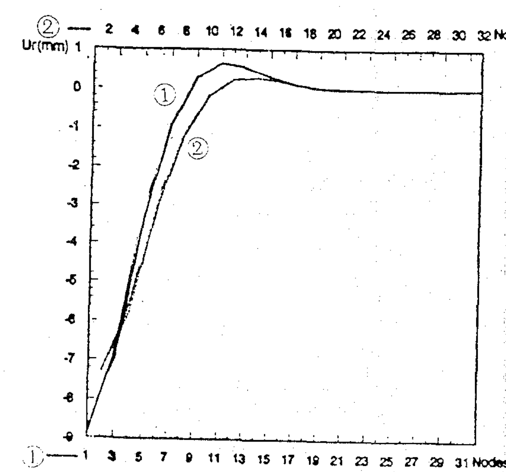

Fig. 3—5 The radial displacements of the outer and internal nodes

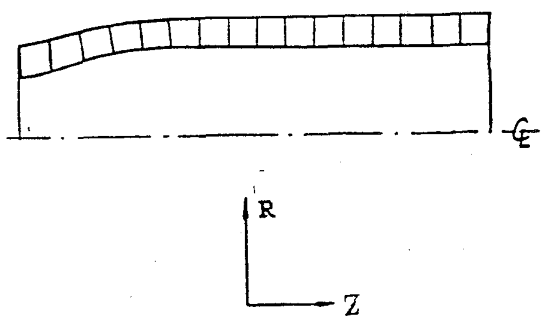

Fig. 3—6 The armature deformation in the 1—stage coilgun

greater than the average value, is adopted in our calculation, the calculated electromagnetic forces are greater than the actual values. Thedeformation results in Fig. 3—5 may be slightly larger than actual values but they essentially show the mechanical performance of the armature. The test and theoretical analysis show that a liner should be adopted in order to increase the mechanical strength and rigidity of the armature.

CONCLUSION

1. For the 3—stage reconnection coilgun in this paper the results of the simulation analysis using concentrated parameters equations (1) agree well with those of the test.

2. The AC and DC modes of the driver coils have different advantages respectively. The AC mode gains higher efficiency of energy transformation and muzzle velocity. The acceleration fluctuation is lower in the DC mode.

3. The mechanical strength of the aluminium alloy cylindrical armature is insufficient although it has, in this 3—stage coilgun, a 10mm thick wall. A liner should be adopted to increase it.

REFERENCE

[1] J. L. He, E. Levi, Z. Zabar, and Birenbaum, Concerning The Design of Capacitively — Driven Induction Coilgun, IEEE Trans. on Plasma Science, June 1989, Vol. 17, No. 3, pp. 429—438

[2] D. M. Wang, Y. J. Wang, Y. M. Zhu and J. J. Chen, Calculation of Inductance and Its Gradients in Coilguns, Proceedings of the 1994 International Conference on Computational Electromagnetic and Its Applications, Nov. 1—4, 1994, Beijing, China, pp220—223

[3] M. Cowan, M. M. Widner, E. C. Cnare, B. W. Duggin, R. J. Keye and J. R. Freeman, Exploratory Developmant of the Reconnection Launcher 1986—1990, IEEE Trans on MAG; 1991; 27(1), pp. 563—567

[4] Y. M. Zhu, G. M. Wei and D. M. Wang, The analysis of the Transferring the AC Work Fashion to DC of the Coilgun, 8th EML Sym. Apr. 21—24, 1996, Baltimore, U. S. A.